EXPERIMENTAL ANALYSIS OF CDMA SYSTEM PERFORMANCE IMPROVEMENT WITH TRIANGLE PIFA ANTENNA ARRAY IN AN ACADEMIC CAMPUS

Arismar Cerqueira S. Jr. and L. C. Kretly

Abstract - The adaptive antenna arrays have been regarded as the key solution for increasing the spectral efficiency and improving the system performance in 3G and 4G mobile communication systems. Although the implementation of adaptive antennas is mainly investigated in the Base Transceiver Station, BTS, it is interesting to evaluate their performance at the mobile level. The purpose of this paper is to analyze the results of the propagation measurements carried out at 1.9GHz in a CDMA system with Triangle PIFA Antenna Array, not only in the signal transmission, but also in its reception, with the aim of acquiring a suitable prototype, that can be applied to adaptive antenna systems. Different wireless environments, such as suburban, indoor and woody were exploited, with line-of-sight (LOS) and non-line-of-sight (NLOS) scenarios. The analysis of results was based on attenuation prediction and comparisons with the received signal by a traditional monopole that is still very used in handsets. Besides, this work describes the Triangle PIFA Antenna Array and monopole prototypes and analyzes their main features in terms of return loss and radiation pattern.

Keywords: Adaptive antenna arrays, attenuation, propagation measurements, PIFA, CDMA, steering.

Resumo - Os arranjos de antenas adaptativos têm sido reconhecidos como a solução chave para aumento da eficiência espectral e para melhora do desempenho dos sistemas de comunicações móveis das próximas gerações, 3G e 4G. Embora a implementação das antenas adaptativas seja principalmente investigada nas ERBs, Estações Rádio Base, é interessante avaliar o seu desempenho na estação móvel, com a finalidade de alcançar um protótipo que possa ser aplicado em sistemas de antenas adaptativos. O objetivo deste artigo é analisar os resultados das medidas de propagação de um sistema CDMA, centrado em 1,9GHz, uque utiliza um arranjo triangular de antenas PIFA, tanto na transmissão quanto na recepção do sinal. Foram analisados diferentes ambientes de propagação, tais como suburbanos, *indoors* e arborizados, com e sem linha de visada. A análise dos resultados foi baseada na predição de atenuação e em comparações com o sinal recebido por um monopolo tradicional, que é ainda muito utilizado em aparelhos celulares. Além disso, esse trabalho descreve os protótipos do monopolo e do arranjo triangular de antenas PIFA, e analisa seus principais parâmetros em função da perda de retorno e do padrão de radiação.

Palavras-chave: Arranjos de antenas adaptativos, atenuação, medidas de propagação, PIFA, CDMA, guiamento do feixe de radiação.

1. INTRODUCTION

The mobile radio channel places fundamental limitations on the performance of wireless communication systems. The path between the transmitter and the receiver can vary from simple LOS to one that is severely obstructed by buildings, mountains and foliage. Unlike wired channels, which are stationary and predictable, radio channels are extremely random and do not offer easy analysis. Even the speed of motion impacts how rapidly the signal level fades, when a mobile terminal moves in space.

In recent years, the demand for mobile communication system has increased in a significant way. Current mobile communication systems have employed sectorization to reduce the jammer and increase their capacity. Increasing the amount of sectorization reduces the jammer seen by the desired signal. A drawback of this technique is that its efficiency decreases with the number of sectors, due to the antenna pattern overlap [1]. Moreover, the number of handoff are proportional to the number of sectors.

Until the second generation of mobile communication systems, the engineers and researches attention was concentrated on developing new protocols, codes and modulations. On the other hand, in the next generations, 3G and 4G, the antennas will play an important role in system performance. The technological progress in this area has a multidisciplinary feature that includes the analysis of new antenna array geometries, design of efficient switch and phase shifter devices and development of optimization algorithms to be applied in the received signal. This work was focused on antenna array and phase shifter designs.

The adaptive antenna arrays have been proposed to reduce multipath fading of the desired signal and to suppress the co-channel interference, through the steering of the main lobe [2]. An adaptive antenna array can adjust and update its radiation pattern to enhance the desired signal, to cancel or reduce interference and to collect correlated multipath, as shown in figure 1(a) [3].

The great contribution of this work is the creation of a triangle antenna array with PIFA, Planar Inverted-F Antennas, elements [4]. The PIFA antenna satisfies the requirements of

Arismar Cerqueira S. Jr. is PhD student of Scuola Superiore Sant'Anna di Studi Universitari e di Perfezionamento, Italy. L.C. Kretly is with Microwave and Optics Department, DMO, Electrical and Computer Engineering Faculty, FEEC, State University of Campinas, UNICAMP, Campinas, SP, Brazil. E-mails: arismar.cerqueira@cnit.it, kretly@dmo.fee.unicamp.br. Review coordinated by Denise Consonni (Area Editor). Manuscript received June/09/2003, reviewed Sept/26/2003, accepted Dec/02/2003.

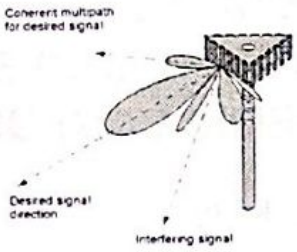

(a) Adaptive antenna array concept.

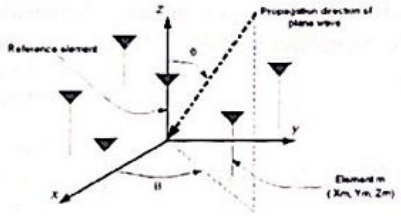

(b) Azimuth (θ) and elevation(ϕ) directions.

Figure 1. Adaptive antenna array concept and its coordinate system.

terminals design of mobile communication systems, such as a reduced size, cost and power consumption. Furthermore, it has other advantages, as high gain and directivity in comparison to the commonly used normal-mode helical antennas [5].

The dimension of the constructed array can be considered large for handsets, however it can be applied in a BTS and it is a serious candidate for being incorporated into wearable systems [6], which are coming up, such as wearable computers or portable communication system and the associated antenna arrangement.

A commercial electromagnetic simulation tool, ZELAND IE3D [7], was used to evaluate and optimize the antenna array design for applications at 1.9GHz. This software solves the current distribution on 3D and multilayer structures of general shape, based on method-of-moments.

2. DEVICE DESIGN AND RESULTS

This section presents the monopole antenna and antenna array design methodologies, including the project of quadrature hybrid, that has been used as phase shifter of antenna array. Furthermore, their simulated and measured results are presented.

2.1 MONOPOLE

Wire antennas, linear or curved, are some of the oldest, simplest, cheapest and, in many cases, the most versatile for many applications. In practice, a wide use has been made of a quarter-wavelength monopole ($l = \lambda/4$) mounted above a ground plane, that is equivalent to a half-wavelength dipole ($l = \lambda/2$). The imaginary part of input impedance of a linear monopole can be eliminated by making the total length, l, of the wire slightly less than n integral number of half-lengths(i.e., l sight less than $n\lambda/4$, n=1,2,3,4...) [8]. In our case, we had used the software Zeland IE3D to optimize it, in function of return loss(S_{11}), and we have gotten an optimized length l=39.9cm at 1.9GHz, that represents $l = 0.238\lambda$, instead of $l = 0.25\lambda$.

Thick cylindrical monopoles are considered broadband whereas thin monopoles are more narrowband. One method by which its acceptable bandwidth can be enlarged is to decrease the l/d radio, where d is the monopole diameter. For example, an antenna with l/d=5000 has a bandwidth of about 3%, whereas an antenna of the same length but with l/d=260 has a bandwidth of about 30%. In general, it has been noticed that for a given length wire its impedance variations become less sensitive as a function of frequency as the l/d ratio decrease [8]. Then broadband characteristics may be obtained by increasing the diameter of a given wire. The optimized diameter of prototype is d=1.0mm. The prototype was constructed on a circular ground plane of 15.0cm in diameter, as shown in figure 2(a).

The S_{11} parameter has been measured in a Network Analyzer, HP 8714ET, with the aim of checking the simulated return loss parameters. Figure 2(b) shows the comparison between measured and simulated return loss of constructed monopole antenna. This result proves that the monopole antenna has been well designed, because the discrepancy between simulated and measured S_{11} is only 0.05%. Beside, it provides a dip equal to -29.61 dB and 381.006 MHz bandwidth, which represents 20.05%. These differences are expected because simulation was done without ground plane. The chosen criterion for operation bandwidth was S_{11} less or equal to -10.0 dB, because in these cases 90% of the antenna input power is radiated.

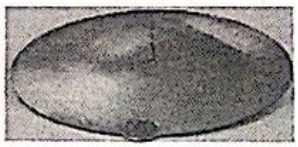

(a) Prototype.

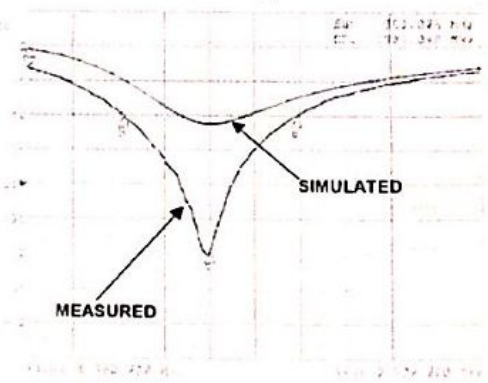

(b) Return loss results.

Figure 2. Monopole prototype and its return loss results.

Monopole has an omnidirectional radiation pattern. It is essentially unaffected by the wire thickness in regions of intense radiation. However, if its radius is increased, the minor lobes diminish in intensity and nulls are replaced by low-level radiation. Figure 3(a) shows its 3D radiation pattern, whereas figures 3(b) and 3(c) show its 2D pattern in the maximum directions of azimuth and elevation plane, ($\theta = 5°, \phi = 170°$), respectively. The simulated directivity and efficiency are, respectively, D= 1.88dB and $\eta = 70.88\%$, thus the simulated gain is approximately G=0.39dBi.

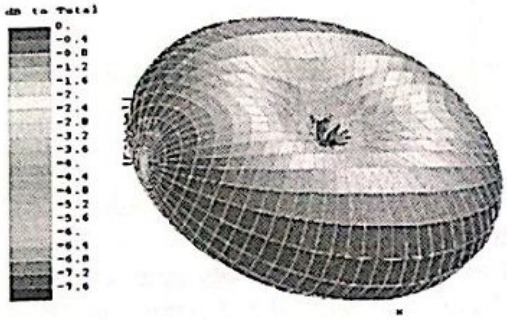

(a) 3D radiation pattern.

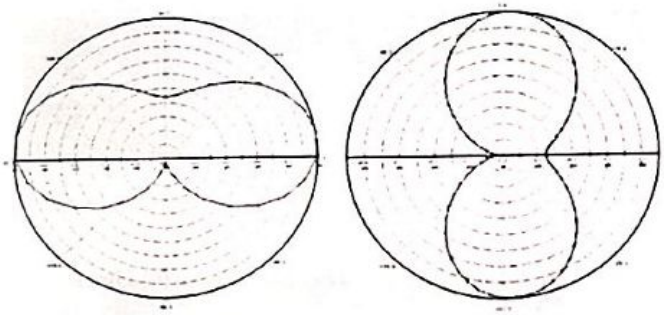

(b) 2D radiation pattern in azimuth plane at $\theta = 5°$.

(c) 2D radiation pattern in elevation plane at $\phi = 170°$.

Figure 3. Monopole radiation patterns.

2.2 TRIANGLE PIFA ANTENNA ARRAY

This subsection is divided into three parts: the first describes the design of PIFA element and its results, the second part presents the quadrature hybrid, which has been used as a phase shifter of antenna array, and, finally, the third part reports the design methodology of triangle PIFA antenna array (TPAA) and its characterization in function of return loss and steerable radiation pattern.

2.2.1 PIFA ELEMENT

The PIFA antennas are like quarter-wave monopole antennas, but they are folded coplanar with the ground plane and stretched to form a plate, as shown in figure 4(a). The side profile looks like an inverted F figure, as shown in figure 4(b).

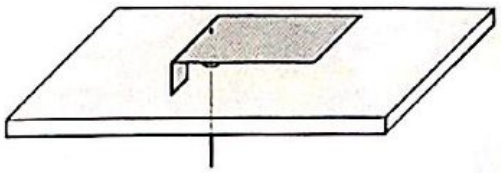

(a) PIFA general view.

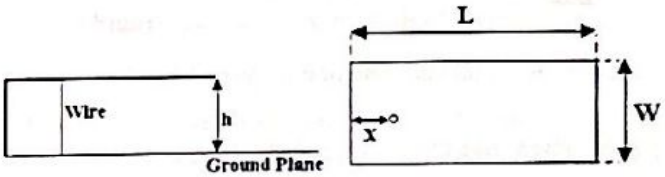

(b) PIFA side view. (c) PIFA top view.

Figure 4. PIFA Antenna Geometry. Dimensions: L=34.0mm, W=12.0mm, h=7.0mm, X= 5.6mm

The width W and the length L of the PIFA determine the resonance frequency, which is approximately given by [9]:

$$f_r = \frac{c_o}{4\alpha(W + L)} \tag{1}$$

where c_o is the velocity of light and α is a constant approximately equal to 0.9. The antenna matching can be controlled by the distance of feeding line, from the shorted edge of the PIFA [10]. Figure 5 shows the simulated return loss of PIFA antenna, with its operating bandwidth.

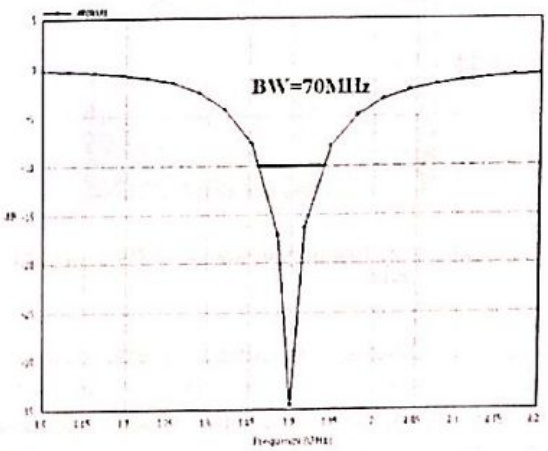

Figure 5. Simulated return loss of PIFA element.

The PIFA element has presented simulated directivity D=3.99dB, 3dB Beam Width equal to 83.48°, efficiency $\eta = 60.78\%$ and radiation pattern, as shown in figure 6

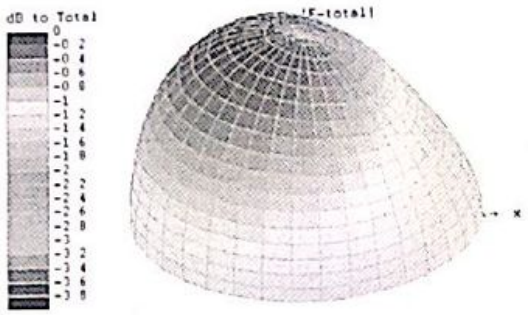

Figure 6. simulated radiation pattern of PIFA element.

2.2.2 QUADRATURE HYBRID

A quadrature hybrid is a four-port directional coupler, as shown in figure 7(a). In general, they are built of microstrip or stripline, as shown in figure 7(b). The great contribution of this work is that hybrid and the TPAA use the same ground plane.

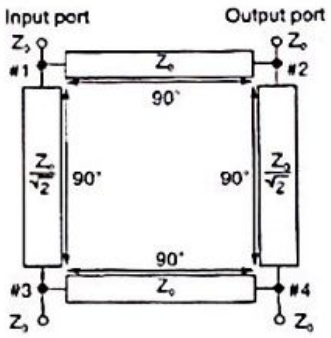

(a) Quadrature Hybrid model.

(b) Constructed quadrature Hybrid.

Figure 7. Quadrature hybrid.

The prototype was built on a fiber glass substrate with dielectric constant ϵ_r=4.8 and thickness equal to 1.6mm. The arm lengths are $\lambda/4$ and their widths are 2.88mm(Z_o) and 5.20mm($Z_o/\sqrt{2}$), which are calculated in accordance to [11].

In the ideal case, power incident on any port is divided equally between two other ports with a 90°phase difference, as shown in the simulated result of figure 8, and the fourth port is isolated. Figure 8(b), measured results of S_{S21} and S_{S31} phases, shows unexpected phase shifts due to parasite elements of ground plane, array elements and SMA connectors.

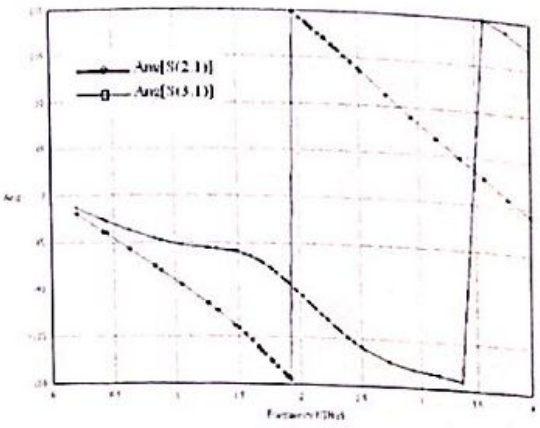

(a) Simulated S_{21} and S_{31} angles.

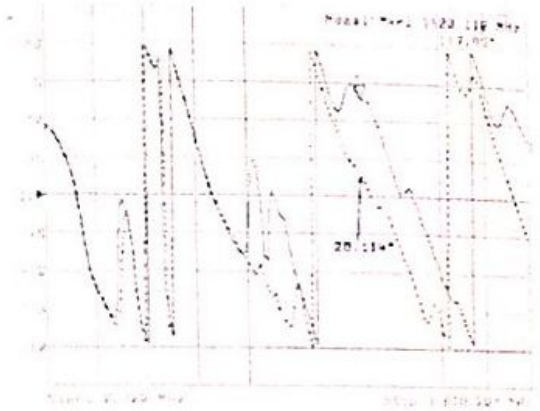

(b) Measured S_{21} (solid line) and S_{31} (dashed line) angles.

Figure 8. Simulated and measured S_{21} and S_{31} angles.

The output ports will always be on the opposite side o the junction from the input port, and the isolated port wil be the remaining port on the same side of the input port. I is possible to see this isolated port, not only in figure 9 by the 3D average current density, but also in figure 10 by S_{21} measurements.

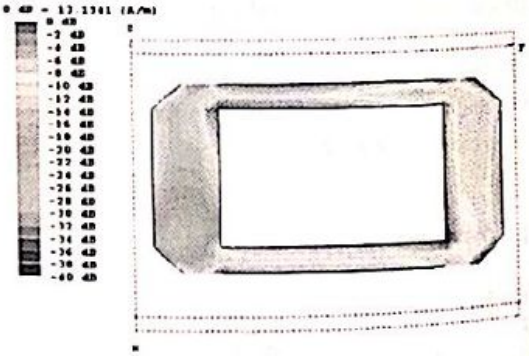

Figure 9. Simulated 3D average current density.

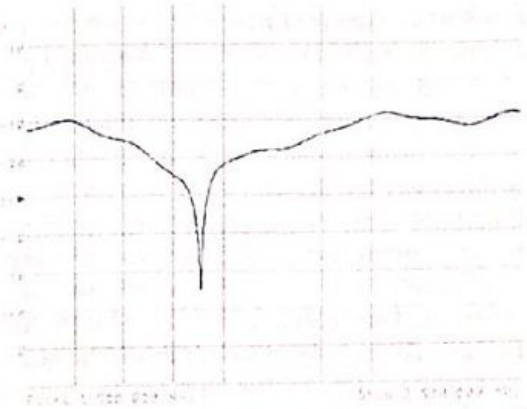

Figure 10. S_{41} measurements.

2.2.3 ARRAY DESIGN AND RESULTS

The antenna array is formed by three identical elements, forming a triangular geometry, as shown in figure 11. The array spacing was chosen $\lambda/2$, because the grating lobes appear in the antenna radiation pattern if this spacing is greater that $\lambda/2$, where λ is the signal wavelength [12].

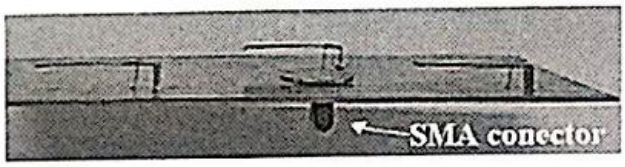

(a) Side view.

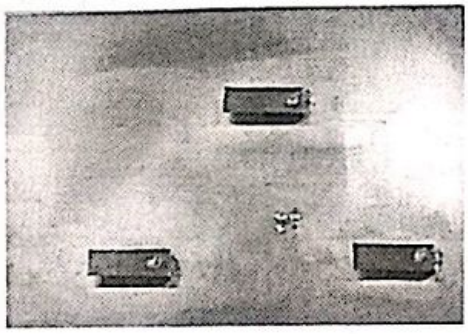

(b) Top view.

Figure 11. Constructed TPAA.

The antenna arrays consider that the desired and interference signals arrive from different directions. The radiation pattern is configured to match the signals from different elements, as shown in figure 12. To reduce the fading and cochannel interference, a diversity system processes three inputs signals, $X_1(t)$, $X_2(t)$ and $X_3(t)$ to create an improved signal $X_c(t)$. The signal improvement depends on the cross correlation and relative signal strength levels between the three received signals [13].

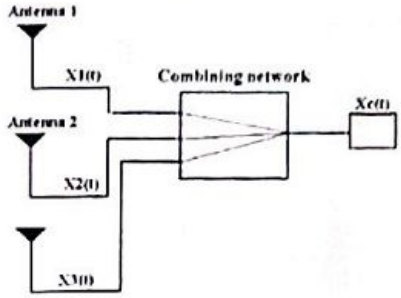

Figure 12. Adaptive Array for 03 elements.

In combining network, weights are attributed to each array element in accordance to the environment, then the feeding intensity and phase can be changed. With these different feeding schemes the radiation pattern can be configured in real time, with the help of control algorithms, which are able to determine the direction of the arrival (DOA) of electromagnetic wave and to suppress the interference, thus the beam is optimized only at the subscriber's direction. Therefore the reuse cell is improved and the signal-to-noise ratio, SNR, is maximized.

The PIFA array was simulated with an infinite ground plane, on a fiber glass substrate with dielectric constant ϵ_r=4.8 and the thickness equal to 1.6mm. Figure 13 shows the comparison between simulated and measured S_{11} of PIFA array.

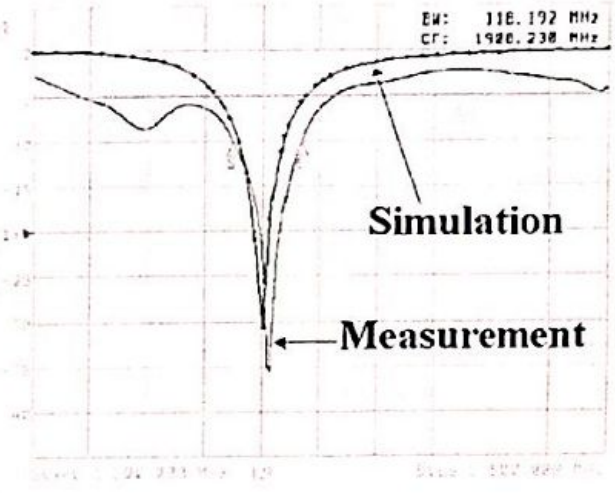

Figure 13. Measured and simulated return loss.

The analysis of the scattering parameter S_{11} shows the prototype has been well designed, because the discrepancy between simulated and measured S_{11} is only 0.4%. Moreover, it provides a bandwidth BW= 118.192MHZ, which represents an improvement of 68.85% in comparison with a PIFA element.

Figure 14 shows the influence of feeding phases (α_i), when the elements 1 and 2 are kept fed and the delay phase is changed, resulting in different 3D radiation patterns. Then the PIFA array can steer the main lobe without varying the fed elements.

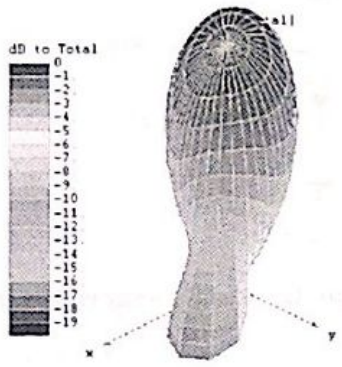

(a) $\alpha_1=\alpha_2=0°$

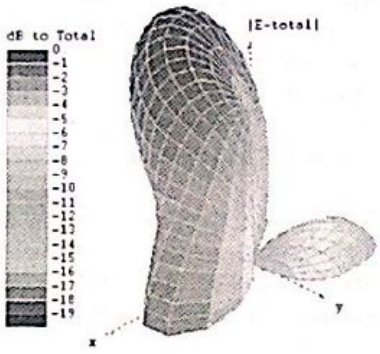

(b) $\alpha_1=0°$and $\alpha_2=90°$.

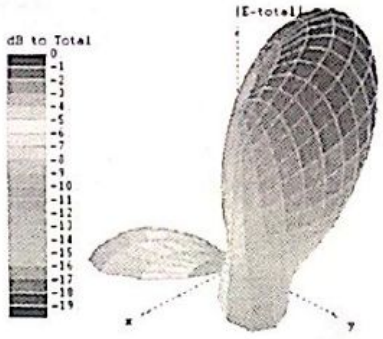

(c) $\alpha_1=90°$and $\alpha_2=0°$.

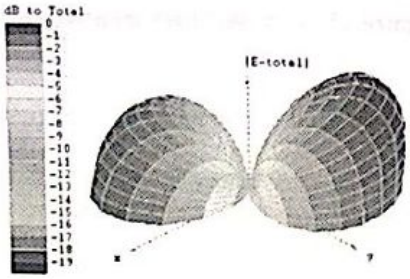

(d) $\alpha_1=0°$and $\alpha_2=180°$.

Figure 14. 3D Radiation pattern with the elements 1 and 2 fed with different phases.

The radiation pattern of figure 14(a) is the most concentrated, with directivity D = 8.24 dB . Whereas figures 14(b) and 14(c) patterns have similar electric features, but the lobe directions are approximately opposite. Finally, figure 14(d) pattern shows two symmetric and identical lobes, for this reason the directivity has decreased to D = 6.29dB.

The adaptive array processing is very useful to capacity and the range improvement [12], because it is important to find users in cell, with the aim of steering the main lobe in their direction. This technique is called SDMA, Space Multiple Division Access. By means of this technique, the same channel can be used more than once inside of the same cell. The bias diversity can be used to distinguish two very close users in a cell.

Based on different feeding schemes, some array configurations have been simulated to exemplify its steerable features, not only in azimuth plane but also in elevation plane. Figure 15 presents the beam steering in some directions of elevation plane. Whereas figure 16 shows some 2D radiation pattern examples in azimuth directions, with a high directivity and without the presence of secondary lobes.

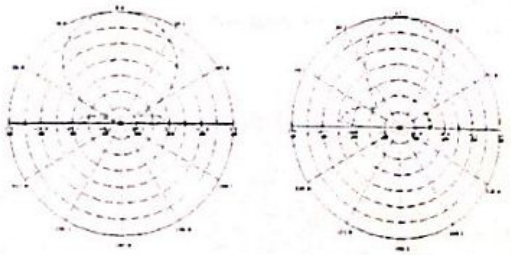

(a) ϕ=0°. (b) ϕ=5°

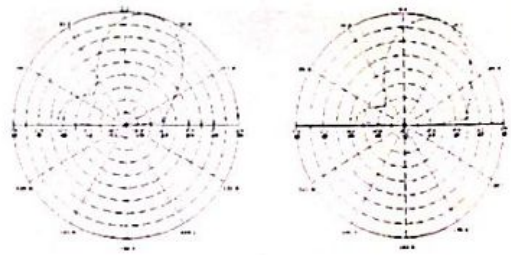

(c) ϕ=15° (d) ϕ=25°

Figure 15. 2D Radiation pattern in different directions of elevation plane.

3. EXPERIMENT DESCRIPTION AND MEASUREMENT PLAN

A set of propagation measurements was conducted at the State University of Campinas (UNICAMP) campus, in the Electrical Engineering Faculty (FEEC) neighborhoods, where different propagation situations can be explored, such as LOS, obstacle attenuation, woody and indoor environments. The purpose of this work is to analyze the performance improvement with Triangle PIFA Antenna Array in

different environments, not only in signal transmission, but also in its reception. The Triangle PIFA Antenna Array was used to transmit the CDMA signal. It has been placed on a 7.6m tall tower, as shown in figure 17(a). In this tower, there is a NITEC Robot Positioner EPR-203 servomechanism, that is responsible for changing the directions of azimuth and elevation planes. It has been controlled by Labview software.

The CDMA signal has generated, at 1.9GHz, in laboratory with Agilent E6380A CDMA Cellular/PCS Base Station Test Set and amplified by HUGHES Traveling Wave Tube (TWT) Amplifier 1177H L Band , as shown in figure 17(c). The measured gain of this amplifier at 1.9GHz is equal to 38.87dB and the attenuation due to cables, connectors and adapters is $\alpha = 10.19dB$. Then it is possible to calculate the effective radiated power in function of this measured gain, the output average power P_{tx} of CDMA generator and transmission antenna gains.

The reception testbed simulates someone, who is making a cellular phone call, as shown in figure 17(b). In this testbed, the CDMA signal is received by monopole or by triangle PIFA antenna array and analyzed by Spectrum Analyzer HP 8593E. The measured results are saved in a computer, as shown in figure 17(d). A GPIB-Serial converter, National Instruments GPIB - 232CT-A, has been used to convert the data from spectrum analyzer.

(a) Transmission antenna tower.

(b) Reception prototype.

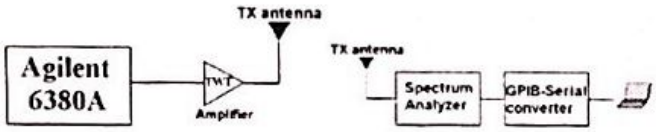

(c) Transmission feeding scheme.

(d) Reception feeding scheme.

Figure 17. Reception prototype and feed schemes.

Figure 18 shows the map of UNICAMP campus with a circle in the coverage area. To evaluate the CDMA system performance improvement with Triangle PIFA Antenna Array , four different situations have been chosen:

- Link with Line-of-sight (LOS), as shown in figure 19(a).
- A suburban environment, as shown in figure 19(b).
- A woody environment, as shown in figure 19(c).
- An indoor environment, as shown in figure 19(d).

Figure 18. Map of UNICAMP campus with the coverage area.

(a) Link with LOS.

(b) Suburban environment.

(c) Woody environment.

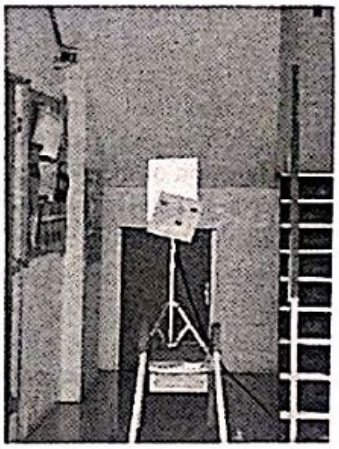

(d) Indoor environment.

Figure 19. Different environments used in the experiment.

4. PREDICTION ATTENUATION AND MEASURED RESULTS

Radio propagation is affected by many factors, including frequency, distance, antenna heights, curvature of the earth,

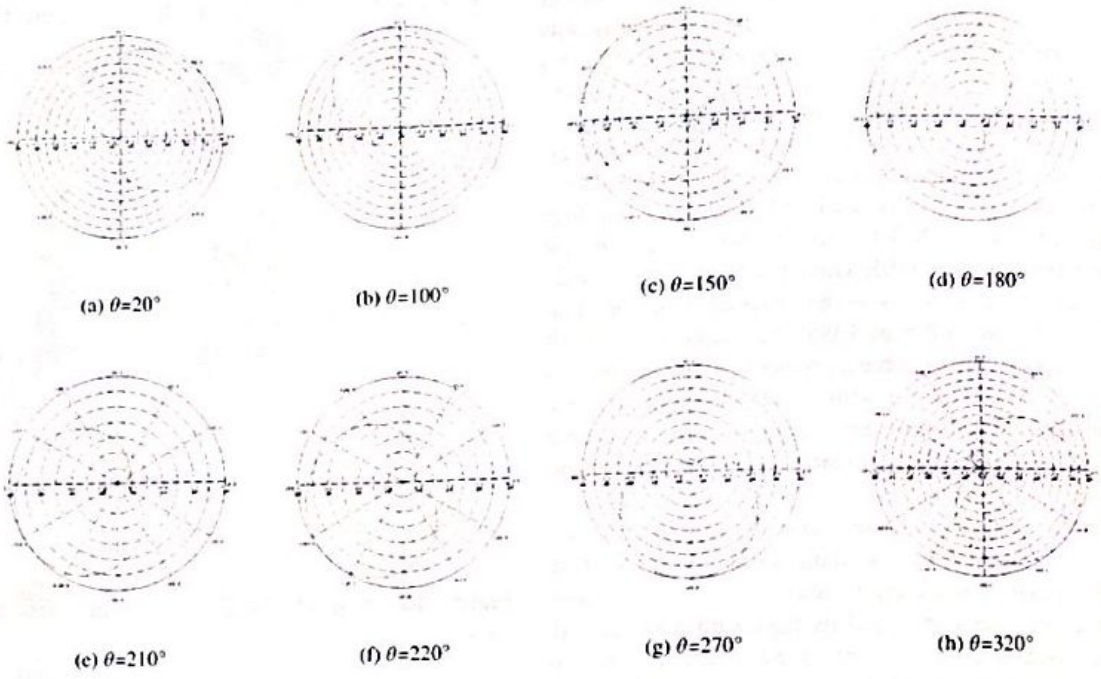

Figure 16. 2D Radiation pattern in different directions of azimuthal plane.

atmospheric conditions and presence of hills and buildings. Mobile-radio signals are also affected by various types of scattering and multipath phenomena, which can cause severe signal fading, that is compounded by the effects of long-term fading and short-term fading, which can be separated statistically [14].

4.1 LINK WITH LOS

The first case is the simplest one, in which there is an unobstructed line-of-sight(LOS) between the reception testbed and the transmitter antenna. In this case, the free space propagation model can be used to predict the received signal strength. This model predicts that the received power decays as a function of the T-R separation distance d. The received power is given by the Friis free space equation, that has been modified as shown in equation 2:

$$P_{RX} = P_{TX} + 27.6 - 20\log d - 20\log f + G_{TX} + G_{RX} \quad (2)$$

where P_{TX} is the transmission power (dBm), d is the T-R separation distance (m), f is the frequency (MHz), and G_{TX} and G_{RX} are the transmission and reception antenna gains, respectively, (dBi).

The simulated gains of monopole and TPAA are 0.39 dBi and 6.30 dB [4], respectively. Since the CDMA average P_{TX} was equal to 0dBm, the predicted P_{RX} of monopole and TPAA are, respectively, -38.26dBm and -33.62dBm, whereas the measured P_{RX} are -41.22dBm and -34.0dBm, as shown in figure 20. Monopoles have an omnidirectional radiation pattern, so it is more sensitive to reflections than TPAA, that has a directional radiation pattern, for this reason the monopole case has presented a relative big discrepancy between its measured and predicted powers. The discrepancy between measured and predicted powers of TPAA is only 0.38dBm, that proves the high directivity of this array and that the prototype simulated gains are close to their real gains.

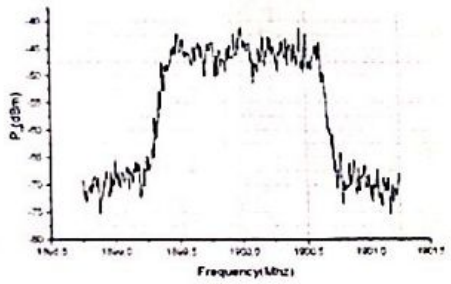

(a) P_{RX} of monopole.

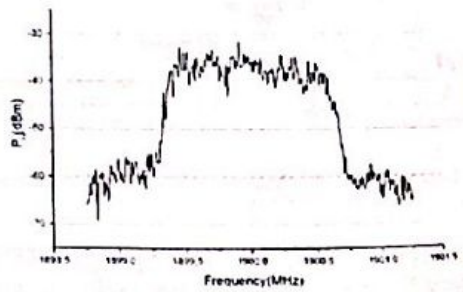

(b) P_{RX} of TPAA.

Figure 20. Measured P_{RX} in link with LOS.

At this site, it has carried out a measurement setup of electric field in open field. So that, the NITEC servomechanism has been used to obtain the 2D azimuthal radiation pattern

at the elevation direction ϕ=5°. An algorithm has been designed, in Labview, to get the average power by step of 5°at azimuth direction, θ. The elements 02 and 03 of TPAA have been fed with phase delay equal to -90°. Figure 21 shows the comparison between measured and simulated radiation pattern. It is very easy to realize that their nulls have tallied at the same azimuth directions, so it is possible to conclude the simulation tool is suitable to predict and analyze the steerable features of antenna arrays.

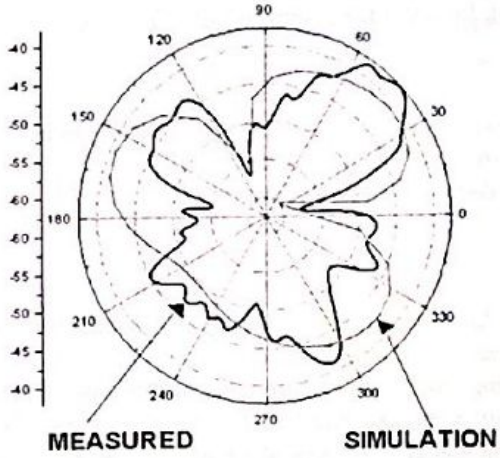

Figure 21. TPAA measured and simulated radiation pattern at ϕ=5°.

4.2 WOODY ENVIRONMENT

In the second case, the effects of vegetation media have been explored on planning and design of radio links at 1.9GHz. Shielding and scattering of microwave signals caused by vegetation are important factors in the planning of microwave radio links. Propagation loss, through a volume of vegetation, has applications wider than that specifically associated with site shielding in which an available screen may be used to provide shielding from interference.

A traditional approach to meddle the additional loss caused by propagation through vegetation assumes that this loss increase exponentially with the distance through foliage. In the model, based on theory of radiative energy transfer for attenuation and scatter predictions, the vegetation medium is treated statistically homogeneous random medium of discrete, loss and scatterers [15]. But it has computational complexity and requires some specific data of the vegetation site. For this reason, the International Telecommunications Union (ITU-R) model has been used to predict the additional attenuation in this case [16]. This model is applicable in the frequency range from 200 MHz to 95 GHz and expresses the attenuation L in dB due to vegetation, in excess to that of free space, as:

$$L_v = 0.2 f^{0.3} d^{0.6} \quad (3)$$

where f is the frequency (MHz) and d is the vegetation average depth(m).

A set of propagation measurements has been conducted in a woody region next to the Electrical Engineering Faculty. The reception testbed has been placed at θ=330°of azimuthal plane. For this reason, the elements 1 and 3 had been fed with

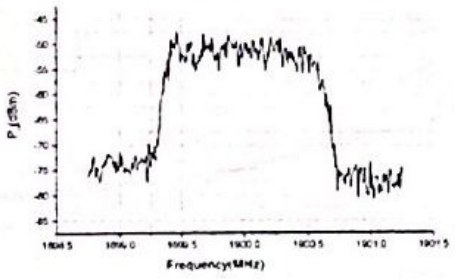

(a) P_{RX} of monopole.

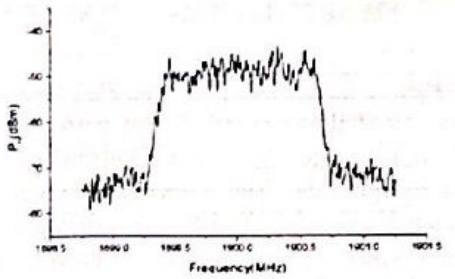

(b) P_{RX} of TPAA.

Figure 22. Measured P_{RX} in a woody environment.

phase delay equal to 90°, so the main lobe has been steered to this azimuth direction.

Considering that the vegetation average depth is 6.0m and remembering that f=1900MHz, the calculated attenuation due to vegetation is $L_v = 5.64dB$. Since $P_{TX} = 0dBm$, the predicted P_{RX} of monopole and TPAA are, respectively, -47.32dBm and -42.97dBm, whereas the measured average P_{RX} are -50.98dBm and -44.28dBm, as shown in figure 22. The discrepancy between measured and predicted powers of TPAA is 1.31dBm. As well as in the first case, the TPAA has improved the system performance.

4.3 SUBURBAN ENVIRONMENT

In the suburban environment, there was a building, with height of 11.0m, between the reception and transmission antennas, and others around it, that is a typical case of out-of-sight link. The total path loss can be expressed in function of three independent terms: the free space loss, the diffraction loss from rooftop to street and the reduction due to plane wave multiple diffraction past rows of buildings [17].

The reception testbed has been placed at direction θ=150°of azimuthal plane. For this reason, the elements 1 and 2 had been fed with phase delay equal to -90°, so the main lobe has steered at this azimuth direction.

There are many prediction models to calculate the path loss in urban and suburban environments [18] [19] [20]. Lee's Microcell Model [14], which is used for distances of less than 1 Km, has been used to predict the attenuation in this environment. Since the distance d=117.73m, it is easy to see, through figure 23, that the building loss is approximately -15dB.

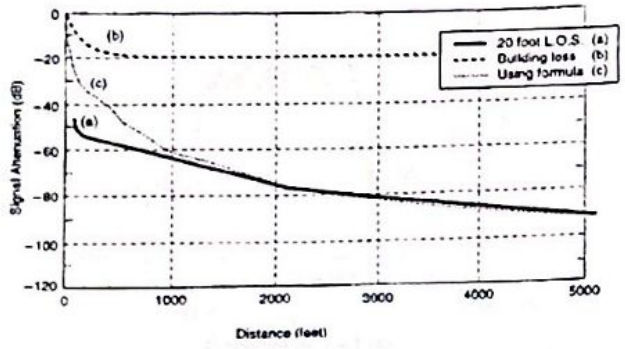

Figure 23. Lee's Microcell Model.

Since $P_{TX} = 0dBm$, the predicted P_{RX} of monopole and TPAA are -59.86dBm and -55.23dBm, respectively, whereas the measured average P_{RX} are -63.74dBm and -55.64dBm, as shown in figure 24. The discrepancy between measured and predicted powers of TPAA is approximately null. Besides, the TPAA has provided an improvement in link quality equal to 8.1dBm. This experiment has proved the adaptive antennas can improve link quality through multipath management.

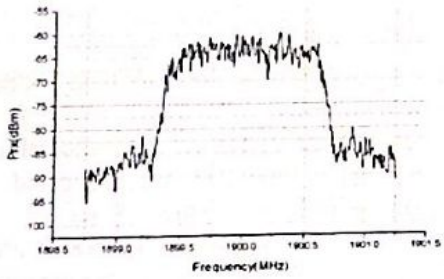

(a) P_{RX} of monopole.

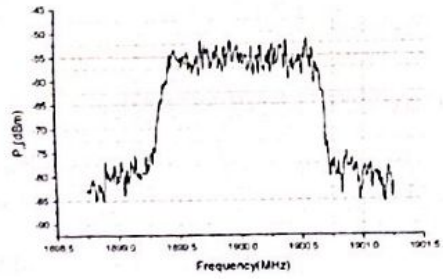

(b) P_{RX} of TPAA.

Figure 24. Measured P_{RX} in suburban environment.

4.4 INDOOR ENVIRONMENT

Finally, in the last case, the reception testbed has been placed inside a FEEC building, 45.5m wide, with the aim of exploiting an indoor environment. In this case the signal has been obstructed by rooms, then a new component needs to be added to the path loss.

The transmitter and reception testbed have formed an angle θ=240°in this case, for this reason the elements 02 and 03 have been fed with phase delay equal to -90°for steering the main lobe at this azimuth direction. It is necessary to consider two components to predict the attenuation: the first due to free space(L_{d1}) and the second due to indoor propagation(L_{d2}), where d_1=70.5m is the distance between the first room intersection and transmitter and d_2=23.0m is the distance between the first room intersection and receiver. The first component is calculate by Frii's equation and the second, for d_2 in feet, is given by [21]:

$$L_{d2} = m_{room} \log d_2 \tag{4}$$

where m_{room} is the room slope, that is 20 in this case, because the total distance, $d = d_1 + d_2$, is within the Fresnel's Zone, that is given by distance [14]:

$$D_f = \frac{4h_1h_2}{\lambda} \tag{5}$$

where h_1 and h_2 are the distances of transmission and reception antennas, respectively.

Then, since $P_{TX} = 5.0dBm$ in this case, the predicted P_{RX} of monopole and TPAA are, respectively, -70.59dBm and -65.95dBm, whereas the measured average P_{RX} are -68.63dBm and -63.46dBm, as shown in figure 25. Surprisingly, the measured P_{RX} is better than the predicted value. It is justified by the standard deviation of this method, that is within 3.0 dB [21]. It is easy to realize that CDMA signal, received by TPAA is much more accurate than the signal received by monopole. As well as in the other cases, the TPAA has overcome the monopole and attended performance improvement expectations.

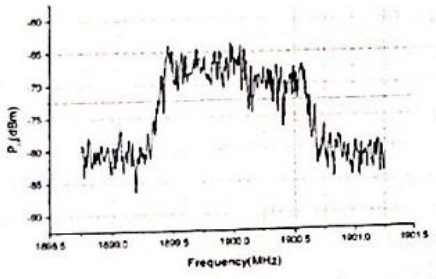

(a) P_{RX} of monopole.

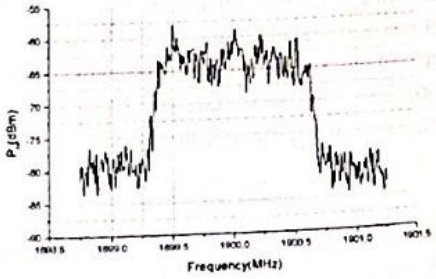

(b) P_{RX} of TPAA.

Figure 25. Measured P_{RX} in indoor environment.

5. CONCLUSION

The experimental investigation and attenuation predictions of CDMA systems performance improvement with TPAA, in different environments, have been proposed and analyzed, not only in base station but also at the mobile level. This array represents a low cost solution to be applied in adaptive systems, because it has a steerable radiation pattern with high efficiency and gain. These features are quite interesting, since the TPAA can efficiently configure its radiation pattern in accordance to the environment in real time, with the aid of control algorithms. Besides measurements of S_{11} parameter have shown that at 1.9GHz, this triangle array has a suitable bandwidth and excellent dip equal to -35.67 dB.

The TPAA has been configured in accordance to the transmitter and receptor positions with the aim of steering the main lobe at the mobile station direction. Then in all studied environments, the TPAA has overcome the monopole antenna and the attenuation predictions have been satisfied. Measured results have shown that the simulations in terms of steering and gain are coherent and accurate. In the environment with LOS, it has been possible to prove the simulated and the real gains are approximately equal. In a woody environment, the effects of vegetation media on the planning and design of radio links have been analyzed and a suitable ITU-R model has been presented and used to predict the attenuation due to foliage. Whereas in suburban scenario, an improvement link quality equal to 8.1 dB has been noticed, through multipath management. Finally, the last case has been carried out in an indoor environment, where the TPAA has presented an accurate measured CDMA signal, with an improvement in the measured P_{rx} equal to 5.17 dBm.

A measurement setup of radiation pattern in open field has been successfully proposed and its result has proved the used simulation tool is suitable for predict and analyze the steerable features of antenna arrays.

Furthermore, the design methodology of devices, used in the experiments, has been presented, jointly with their simulated and measured results .

ACKNOWLEDGMENTS

This work was partially supported by Ericsson EDB(Ericsson Research Center Brazil) under contract Ericsson/Unicamp UNI.15.

The authors gratefully acknowledge the technical support provided by Electrical Engineer Antonio Marcelo Ribeiro, from UNICAMP, on the project and implementation of the Labview software algorithm, used acquiring data from Spectrum Analyzer.

REFERENCES

[1] Ahmed EL Zooghby, "Potentials of smart antennas in CDMA systems and uplink improvements," *IEEE Antennas and Propagation Magazine*, vol. 05, no. 43, pp. 172–177, Oct. 2001.

[2] L. C. Kretly, Arismar Cerqueira S. Jr., and A. Tavora A. S., "A hexagonal adaptive antenna array concept for wireless communication applications," *IEEE International Symposium on Personal, Indoor and Mobile Radio Communications*, Sept. 2002.

[3] Joseph C. Liberti and Theodore S. Rappaport, *Smart Antennas for Wireless Communications* IS-95 *and Third Generation* CDMA *Applications*, Prentice Hall PTR, 1999.

[4] L. C. Kretly, Arismar Cerqueira S. Jr., and A. Tavora A. S., "Triangle PIFA antenna array prototype for wireless system applications," *IEEE ITS International Telecommunications Symposium*, Sept. 2002.

[5] Koichi Ogawa, Toshimitsu matuyoshi, and Kenji Monma, "An analysis of the performance of a handset diversity antenna influenced by head, hand, and shoulder effects at 900MHz: PartI - effective gain characteristics," *IEEE Transactions on Vehicular Technology*, vol. 50, no. 03, pp. 830–844, May 2001.

[6] Pekka Salonen, Lauri Sydänheimo, Mikko Keskilammi, and Markku Kivikoski, "A small planar inverted-f antenna for wearable applications," *The Third International Symposium*, pp. 95–100, 1999.

[7] Zeland, "IE3D," *http://www.zeland.com*.

[8] Constantine A. Balanis, *Antenna Theory: Analysis and Design*, John Wiley Sons, second edition, 1997.

[9] P.K. Panayi, M.O. Al-Nuaimi, and L.P. Ivrissimtzis, "Tuning techniques for the planar inverted-f antenna," *Electronics Letters*, vol. 37, no. 16, pp. 1003–1004, Aug. 2001.

[10] A.F. Muscat and C.G. Parini, "Novel compact handset antenna," *International Conference on Antennas and Propagation*, , no. 480, pp. 336–339, Apr. 2001.

[11] K. C. Gupta, Ramesh Garg, and Rakesh Chadha, *Computer-aided design of microwave circuits*, Artech, first edition, 1981.

[12] Paul Petrus, *Novel Adaptive Array Algorithms and Their Impact on Cellular System Capacity*, Doctor of philosophy in electrical engineering, Faculty of the Virginia Polytechnic Institute, Mar. 1997.

[13] Koichi Ogawa, Toshimitsu matuyoshi, and Kenji Monma, "An analysis of the performance of a handset diversity antenna influenced by head, hand, and shoulder effects at 900MHz: Effective gain and correlation characteristics," *IEEE Transactions on Vehicular Technology*, vol. 50, no. 03, pp. 845–853, May 2001.

[14] William C. Y. Lee, *Mobile communications Engineering*, McGraw-Hill, second edition, 1997.

[15] M. O. Al-Nuaimi and A. M. Hammoudeh, "Measurements and predictions of attenuation and scatter of microwave signals by trees," *IEE Proc. Microwave Antennas Propagation*, vol. 141, no. 02, pp. 70–76, Apr. 1994.

[16] M. O. Al-Nuaimi and R. B. L. Stephens, "Measurements and prediction model optimisation for signal attenuation in vegetation media at centimetre wave frequencies," *IEE Proc.-Microwave Antennas Propagation*, vol. 145, no. 03, pp. 201–206, June 1998.

[17] Howard H. Xia, "An analytical model for predicting path loss in urban and suburban environments," *IEEE International Symposium on Personal, Indoor and Mobile Radio Communications*, vol. 1, pp. 19–23, 1996.

[18] Lajos Nagy and Béla Nagy, "Comparison and verification os urban propagation models," *IEEE International Symposium on Antennas and Propagation*, pp. 1359–1363, 1994.

[19] Minseok Jeong and Bomson Lee, "Comparison between path-loss prediction models for wireless telecommunication system design," *IEEE International Symposium on Personal, Indoor and Mobile Radio Comm.*, vol. 2, pp. 186–189, 2001.

[20] N. Blaunstein, R. Giladi, and M. Levin, "Characteristics prediction in urban and suburban environments," *IEEE Transactions on Vehicular Technology*, vol. 47, pp. 225–234, Feb. 1998.

[21] William C. Y. Lee and David J. Y. Lee, "Inbuilding prediction," *IEEE International Symposium on Personal, Indoor and Mobile Radio Communications*, vol. 3, pp. 771–775, 1996.

Arismar Cerqueira Sodré Junior was born in Salvador, Bahia, Brazil, in 1978. He received the B. S. degree in electrical engineering from Federal University of Bahia, Brazil, in 2001 and the Master degree in telecommunications engineering from State University of Campinas, Brazil, in 2002. He is currently working on his PhD degree in Scuola Superiore Sant'Anna di Studi Universitari e di Perfezionamento, Italy. From 2000 to 2002, he worked and researched on wireless communication systems and Smart Antennas. His current research interests include Photonic Crystal Fibers, finite element method, optical amplifiers and optical signal processing devices.

Luiz Carlos Kretly is a 1974 graduate of UnB, Universidade Brasília and received his Master and Doctor in E. E. degrees fr UNICAMP in 1992. He was invited researcher at NFFSS in Corn University in 1982. He was Director of the Semiconductor Comp nent Center in UNICAMP from 1988 to 1998 and Director of Equipment Maintenance Center in UNICAMP from 1990 to 199 His areas of work in Microelectronics are Electron Beam Lithog phy and Ion Implantation. He has dedicated himself to the design RF integrated circuits and integrated antennas for cellular telepho He has coordinated a research group in Wireless Communicatio for an RF front-end design. Presently he is professor at Faculda de Engenharia Elétrica e de Computação , FEEC da UNICAMP. is an IEEE member and currently serves as MTT-S Chapter Chair f region 9 South Brazil. His areas of interest include Design of In grated Antennas, HDA High Dielectric Antennas, DVB-DTV, SO System-on-Chip, SOP, System on a Package, MEMS MicroEle tromechanical Systems para RF e NanoEletromechanical Syster NEMS.